Photooxidation and photoaquation of iron hexacyanide in aqueous solution: A picosecond X-ray absorption study

M. Reinhard,[1] T. J. Penfold,[1,2,3] F. A. Lima,[1] J. Rittmann,[1]
M. H. Rittmann-Frank,[1] R. Abela,[3] I. Tavernelli,[2] U. Rothlisberger,[2]
C. J. Milne,[1,3] and M. Chergui[1,a)]
[1]*Ecole Polytechnique Fédérale de Lausanne, Laboratoire de Spectroscopie Ultrarapide, ISIC, FSB, CH-1015 Lausanne, Switzerland*
[2]*Ecole Polytechnique Fédérale de Lausanne, Laboratoire de Chimie et Biochimie Computationnelles, ISIC, FSB, CH-1015 Lausanne, Switzerland*
[3]*SwissFEL, Paul Scherrer Inst, CH-5232 Villigen, Switzerland*

(Received 29 December 2013; accepted 7 April 2014; published online 17 April 2014)

We present a picosecond Fe K-edge absorption study of photoexcited ferrous and ferric hexacyanide in water under 355 and 266 nm excitation. Following 355 nm excitation, the transient spectra for the ferrous and ferric complexes exhibit a red shift of the edge reflecting an increased electron density at the Fe atom. For the former, an enhanced pre-edge transition is also observed. These observations are attributed to the aquated $[Fe(CN)_5OH_2]^{3-}$ species, based on quantum chemical calculations which also provide structural parameters. Upon 266 nm excitation of the ferric complex, a transient reminiscent of the aquated species is observed (appearance of a pre-edge feature and red shift of the edge) but it is different from that obtained under 355 nm excitation. This points to a new reaction channel occurring through an intermediate state lying between these two excitation energies. Finally, 266 nm excitation of the ferrous species is dominated by the photooxidation channel with formation of the ferric complex as main photoproduct. However, we observe an additional minor photoproduct, which is identical to the 266 nm generated photoproduct of the ferric species, suggesting that under our experimental conditions, the pump pulse photooxidises the ferrous complex and re-excites the primary ferric photoproduct. [http://dx.doi.org/10.1063/1.4871751]

I. INTRODUCTION

The solvent is a key factor in most liquid phase chemical and biochemical reactions, and its effects may be classified into two distinct groups: passive or active.[1] Passive solvent effects do not change the quantum states of the solute, but alter their relative energies, as well as modulating the dissipation of energy from the solute to the solvent. Depending on the nature of the interactions (e.g., electrostatic, van der Waals, hydrogen bonding)[2] and on the nature of the solute's quantum states (e.g., valence, charge transfer, and Rydberg),[3,4] trends as a function of the solvent polarity, density, and viscosity are usually observed. While this may lead to changes in the branching ratio of the products, the solvent does not alter the underlying reaction mechanisms. In contrast, for active effects, the solvent molecules take part in the chemical reaction via explicit interactions with the solute, leading to the formation of new molecules.[5]

A case in point for the latter are the ferrous and ferric hexacyanide anions ($[Fe(CN)_6]^{4-}$ and $[Fe(CN)_6]^{3-}$, respectively). In their pioneering work, Shirom and Stein.[6,7] identified two

a)Electronic mail: majed.chergui@epfl.ch

main photoinduced reactions for ferrous hexacyanide in water and found that they exhibit a distinct excitation wavelength dependence. Below 313 nm, the quantum yield of photochemical reactions is dominated by the generation of solvated electrons via the photooxidation channel

$$[Fe(CN)_6]^{4-} \xrightarrow{h\nu} [Fe(CN)_6]^{3-} + e^-_{aq}, \tag{1}$$

which was proposed to occur through charge-transfer-to-solvent (CTTS) states.[7–12] Above ∼313 nm excitation, the products were assigned to the so-called photoaquation channel

$$[Fe(CN)_6]^{4-} + H_2O \xrightarrow{h\nu} [Fe(CN)_6]^{4-*} + H_2O \rightarrow [Fe(CN)_5OH_2]^{3-} + CN^-, \tag{2}$$

that was found to occur in <1 ns, which was the limit of their temporal resolution. The quantum yield for this channel was reported constant between 313 and 365 nm and at pH = 3.8 to 10.5. The authors argued that the $^1T_{1g}$ ligand field (LF) state is the doorway to the aquated species, but did not exclude intersystem crossing to the $^3T_{1g}$ state. They assumed that the aquated photoproduct is $[Fe(CN)_5OH_2]^{3-}$ and found that this species absorbs in the violet, with a maximum at ∼450 nm and a lifetime of several minutes. For $[Fe(CN)_6]^{3-}$, the CTTS states are not observed and Moggi *et al.*[13] assigned the photoproduct, which exhibited no excitation wavelength dependence, to the aquated $[Fe(CN)_5OH_2]^{2-}$ complex. However, in a later study, Horváth and Stevenson[14] concluded that there is an irradiation wavelength dependence. Fuller *et al.*[15] determined a quantum yield for $[Fe(CN)_5OH_2]^{2-}$, $\Phi \sim 0.02 - 0.06$, which is a factor of 5 smaller than for $[Fe(CN)_6]^{4-}$. However, while these studies have revealed information about the two main relaxation channels, they were unable to yield a distinct structural and electronic identification of the photoproducts and their reaction mechanism.

Indeed, the exact mechanism of reaction (2) is often assumed to be a dissociative mechanism, supported by studies on a series of pentacyano(amine)ferrate(II)[16] complexes and a pentacyano(sulphito)ferrate(II) complex.[17] However, strong interactions between the solute and the solvent for these complexes[18,19] raise the question as to whether the photoaquation reaction may be mediated by an electronic interaction with the solvent species. By measuring small but positive activation volumes of the ferrocyanide photoaquation reaction, Finston and Drickamer[20] argued that it proceeds via a dissociative interchange mechanism in which ligand-metal bond breaking and solvent-metal bond making occur simultaneously.[21] This is in line with quantum chemistry calculations which estimated the dissociation energy to be 6.2 eV per Fe-CN bond in the ground state.[22] Although this value may be lower for the excited state, it is still way beyond the 3.4 eV needed to excite the $^1T_{1g}$ state.

In this contribution, we present a picosecond X-ray absorption spectroscopy (XAS)[23,24] study of $[Fe(CN)_6]^{4-}$ and $[Fe(CN)_6]^{3-}$ in water upon 355 nm and 266 nm excitation. For $[Fe(CN)_6]^{4-}$, the transient spectra show a large wavelength dependence in line with the photooxidation and photoaquation reaction channels (reactions (1) and (2)). New features show up in the pre-edge region, which reflect substantial electronic and geometric structure changes, and are analysed using multiple scattering (MS) theory and quantum chemistry calculations.

II. EXPERIMENT AND METHODS

A. Materials

All samples were freshly prepared from potassium ferrocyanide ($K_4Fe(CN)_6 \cdot 3H_2O$) and potassium ferricyanide ($K_3Fe(CN)_6$) obtained from Sigma Aldrich which was dissolved in deionized H_2O. Both, $[Fe(CN)_6]^{4-}$ and $[Fe(CN)_6]^{3-}$ samples, were prepared in unbuffered solutions at a concentration of 45 mM for the 266 nm excitation experiments. In the case of 355 nm excitation, it was 250 mM for ferrocyanide and 120 mM for ferricyanide. The concentration was higher for this case because of the lower absorption coefficients at this wavelength.

B. Experimental setup

Picosecond XAS experiments were carried out at the microXAS beamline of the Swiss Light Source (SLS) facility at the Paul-Scherrer Institute (PSI). A minigap in-vacuum undulator provides X-rays from 4 to 20 keV, which are energy selected by a double crystal, fixed exit Si(111) monochromator.

The experimental setup has already been described in Ref. 25. In short, the pump-laser (10 ps pulses) excited the sample at a repetition rate of 520 kHz, which is then probed by ~70 ps X-ray pulses at 1.04 MHz. The X-ray spot dimensions were 20–50 μm full width half maximum (FWHM) and the laser spot size was slightly larger, 50–70 μm FWHM. The spatial overlap was ensured using a 25 μm thick tungsten pinhole with 50 μm diameter which was placed at the sample position. The transient spectra are obtained by taking the difference between the pumped and unpumped XAS spectra on a pulse-to-pulse basis. The 355 and 266 nm pump pulses are obtained by tripling and quadrupling the fundamental frequency (1064 nm) of the pump laser. All measurements at 355 nm were performed at pump fluences of ~65 mJ/cm^2, whereas the 266 nm excitations were measured at pump fluences of ~40 mJ/cm^2. Sample solutions were flowed at a speed of approximately 5 m/s in a 200 μm or 100 μm liquid jet in the case of 355 or 266 nm excitation, respectively. The jet was tilted by 45° with respect to the incident X-ray beam in order to maximise the fluorescence counts on the detector.

C. Computational details

The energy minimised structures of the investigated complexes (see Table I) were optimised using the ORCA quantum chemistry package[26] at Density Functional Theory (DFT) level within the approximation of the B3LYP* exchange and correlation (*x-c*) potential[27] and the TZVP basis set. During the optimisation, the effect of the solvent was accounted for using the COSMO solvation model[28] and the dielectric constant of water.

Calculations of both the ground and excited state Fe K-edge X-ray near edge absorption structure (XANES) spectra were performed using MS theory implemented in the Finite Difference Method Near Edge Structure (FDMNES) code.[29] Calculations used a self-consistent field potential and were convoluted using an arctangent function accounting for the core-hole lifetime and inelastic losses.[30] The transient spectra were calculated as the difference between the calculated ground and product state spectra, which were scaled to match the experimental intensities. This scaling factor corresponds to the population of excited and/or product species.

The pre-edge spectra were simulated using Time dependent Density functional theory (TD-DFT) adapted for core hole spectra[31] as implemented within the ORCA quantum chemistry package.[26] As before, the calculations were performed using the B3LYP* *x-c* functional[32,33] and a TZVP basis set. The TD-DFT equations were solved for 10 states, within the Tamm-Dancoff approximation[34] and the interaction with the X-ray field was described using the electric quadrupole approximation.[35]

TABLE I. Main structural parameters of the complexes considered in this work. *ax* = axial and *eq* = equatorial with respect to the dissociated ligand.

	$[Fe(CN)_6]^{4-}$	$[Fe(CN)_6]^{3-}$	$[Fe(CN)_5]^{3-}$	$[Fe(CN)_5]^{2-}$	$[Fe(CN)_5OH_2]^{3-}$	$[Fe(CN)_5OH_2]^{2-}$
Fe Ox. state	2+	3+	2+	3+	2+	3+
Fe-C (Å)	1.93	1.95	1.85^{ax}	1.84^{ax}	1.88^{ax}	1.88^{ax}
			1.94^{eq}	1.93^{eq}	1.94^{eq}	1.95^{eq}
C-N (Å)	1.17	1.16	1.17	1.16	1.17	1.16
Fe-O (Å)					2.20	2.05

III. RESULTS

A. Ground state Fe K-edge spectrum

Figure S1[49] shows the iron K-edge XANES spectrum of aqueous $[Fe(CN)_6]^{4-}$ and $[Fe(CN)_6]^{3-}$. For both complexes, the above edges resonances are in agreement with previously reported spectra[36–39] and besides a slight increase in the first peak intensity for the ferricyanide, the main difference between the two spectra is the ∼2 eV shift to higher energies for $[Fe(CN)_6]^{3-}$ reflecting the different oxidation states (Fe^{2+} vs. Fe^{3+}). Previous analysis of the above edge[36,38,40] demonstrated that they are dominated by MS pathways along the linear Fe-C-N bonds reporting Fe-C distances of 1.90 Å and C-N distances of 1.19 Å for the ferrous complex. In the ferric complex, a small (0.01 Å) expansion of the Fe-C distance was reported, while the C-N distance remains constant. These trends are confirmed by our DFT calculated structures shown in Table I.

B. 355 nm photoexcitation

For $[Fe(CN)_6]^{4-}$, 355 nm excitation populates the lowest singlet LF state, $^1T_{1g}$, (Fig. S2(a)[49]), and according to Refs. 6 and 7, the photoinduced changes are expected to relate to the formation of the photoaquated species. Fig. 1(a) shows the experimental transient spectrum 70 ps after photoexcitation. It is characterised by three distinct changes: (i) a new pre-edge feature at 7.113 keV; (ii) a negative feature at 7.15 keV, which corresponds to the second above ionisation resonance in the ground state spectrum; and (iii) a ∼1.0 eV red shift of

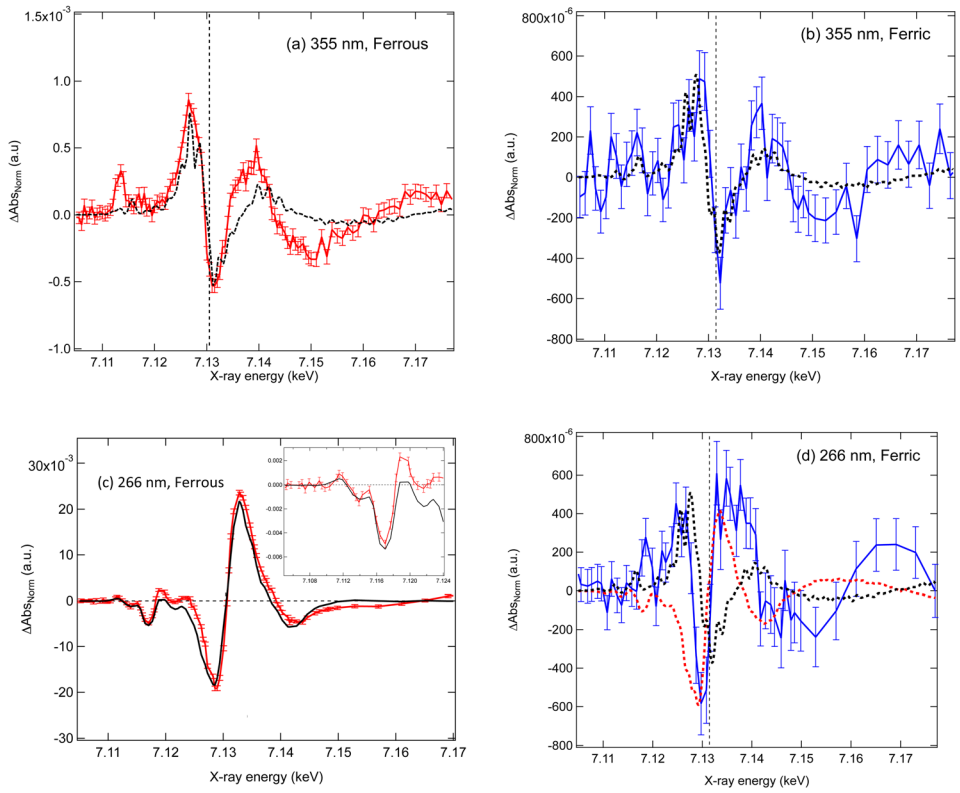

FIG. 1. (a) Transient spectra of aqueous $[Fe(CN)_6]^{4-}$ 70 ps after photoexcitation at 355 nm (a) and 266 nm (c). Transient spectra of aqueous $[Fe(CN)_6]^{4-}$ 70 ps after photoexcitation at 355 nm (b) and 266 nm (d). For figures (a)–(d), the black dashed line represents a shifted ground state spectrum minus the ground state spectrum (*shifted-difference spectrum*) for which the magnitude of the shifts are −1.0 eV in (a), (b) and (d) and + and 1.0 eV (red dashed trace) in (d). The black trace in (c) represents the static difference spectrum between the ferrous and ferric ground-state spectra. The fraction of photo-oxidized species $f \cdot \Phi_{po}(70\,\text{ps}) \sim 3.75\%$. A zoom into the pre-edge region is shown in the inset.

the absorption edge. This is derived by taking the difference of the red shifted ground state spectrum minus itself, which is represented by the black dashed line in Fig. 1(a). The derivative-like profile with positive and negative features at 7.125 and 7.13 keV is well reproduced while deviations above the edge point to a structure change of the system after excitation. The −1 eV shift of the edge hints to an increased electron density on the Fe atom.

Fig. 1(b) shows the transient spectrum 70 ps after 355 nm excitation of $[Fe(CN)_6]^{3-}$, which due to overlapping bands in the absorption spectrum (Fig. S2(b)[49]) populates both the LF $^2T_{1g}$ and the $^2A_{1g}$ Ligand to Metal Charge Transfer (LMCT) states. Although the signal magnitude normalised to the excitation yield[41] is approximately three times smaller than for $[Fe(CN)_6]^{4-}$ in agreement with Ref. 15, the spectrum still exhibits, within the signal-to-noise ratio, an overall similar profile to the $[Fe(CN)_6]^{4-}$ transient (Fig. S3[49]). In particular, the red shift of the absorption edge and the negative feature at 7.15 keV are still observed. As for the ferrous complex, these features are reproduced by taking the difference of the ground state ferric spectrum shifted by 1.0 eV to the red minus the unshifted spectrum. However, because of the poor signal-to-noise ratio, changes in the pre-edge region are difficult to distinguish.

C. 266 nm photoexcitation

For $[Fe(CN)_6]^{4-}$, 266 nm excitation lies in the region of the CTTS states[8–12] (Fig. S2(a)[49]) and given the reported quantum yields for photooxidation ($\Phi_{ox} = 0.5$, Ref. 7) and photoaquation ($\Phi_{aq} \sim 0.1$, Ref. 6), the transient spectrum for $[Fe(CN)_6]^{4-}$ should be dominated by the former with, in particular, a blue shift of the edge. This is indeed the case in Fig. 1(c), which shows the transient spectrum at 70 ps. It is significantly different from the transient at 355 nm excitation (Fig. 1(a)) and is dominated by a ∼2 eV blue shift of the absorption edge (Fig. 1(c)), which results from the conversion of the ferrous to the ferric form (see Fig. S1[49]). This leads to an absorption decrease on the red side of the edge and an increase on its blue side. Besides the transient spectrum also exhibits a number of distinct positive and negative features in the pre-edge region (7.110–7.125 keV).

The 266 nm transient spectrum, assuming only the photooxidised product, is expressed as the difference between the normalised XAS spectra of the ferric $[Fe(CN)_6]^{3-}$ product (A_{po}) and the ground-state (A_{gs}) ferrous $[Fe(CN)_6]^{4-}$ complex scaled by the total fraction of excited species (f) and the quantum yield Φ_{po}

$$\Delta A(E,t) = f(t) \cdot \Phi_{po}[A_{po}(E,t) - A_{gs}(E)], \tag{3}$$

which we refer to as the static difference spectrum. The time-dependence of $f(t)$ reflects the decay of the photoproduct due to electron-ion recombination processes and/or secondary reactions. The black trace in Fig. 1(c) shows the static difference, according to Eq. (3), fitted to the experimental transient by minimising the sum of the square residuals over the spectral range from 7.1 keV to 7.4 keV (see Fig. S4[49]) and using the product $f(t) \cdot \Phi_{po}$ as adjustable parameter. This procedure yields a value of 3.75% for the latter but while the fit is satisfactory, the agreement between static difference and experimental transient spectrum is not optimal and shows deviations in the pre-edge, the edge, and the post-edge regions (Figs. 1(c) and S4[49]). As already discussed, fitting transient spectra is critically dependent on the excitation yield.[42] However, for the time being, we will assume the above value of $f(t) \cdot \Phi_{po}$ to be the optimal one and will discuss it later in terms of its consistency in extracting the second photoproduct of the excitation at 266 nm. The pre-edge features below 7.117 keV are well reproduced (Fig. 1(c), inset) and in the edge-region, the 2 eV shift of the absorption edge to higher energies is also well reproduced. The positive feature just below 7.112 keV corresponds to the $1s \rightarrow t_{2g}$ transition, which is present in the ferric case (see Fig. S1[49]) and arises from the hole created in the t_{2g} orbitals upon photooxidation. The changes between 7.112–7.117 keV arise from the oxidation shift (i.e., to higher energies) of transitions present in both the $[Fe(CN)_6]^{4-}$ and $[Fe(CN)_6]^{3-}$ spectra. The

deviations in Fig. 1(c) have an obvious origin in the fact that there is more than one photoproduct, which should be the aquated species, according to Refs. 6 and 7

If we assume two product channels, Eq. (3) becomes

$$\Delta A(E,t) = f(t) \cdot [\Phi_{po} \cdot \{A_{po}(E,t) - A_{gs}(E)\} + \Phi_{P2} \cdot \{A_{P2}(E,t) - A_{gs}(E)\}]. \quad (4)$$

Φ_{po} and Φ_{P2} represent the quantum yields of the two products. The above derived fraction of photooxidized species ($f \cdot \Phi_{po} = 3.75\%$) may now be used to obtain the transient spectrum of the additional product channel (P2) as

$$f(t) \cdot \Phi_{P2} \cdot \{A_{P2}(E,t) - A_{gs}(E)\} = \Delta A(E,t) - f(t) \cdot \Phi_{po} \cdot \{A_{po}(E,t) - A_{gs}(E)\}, \quad (5)$$

where A_{po}(E, 70 ps) − A_{gs}(E) is the photooxidative channel, i.e., the *static difference spectrum*. The resulting transient spectra for the second product are shown in Fig. 2(a) for time delays of 70 ps and 650 ps. They both exhibit a similar profile with a pre-edge peak at 7.112 keV, which shows an increase at 650 ps. Although the appearance of this peak is reminiscent of the 355 nm transient spectrum of the ferrous species (Fig. 1(a)), the rest of the transient is different to the latter, as can be seen in Fig. S5(b).[49] This is surprising in view of the reports concerning the generation of the aquated species under 266 nm excitation.[6,7] We will come back to this point after presenting the 266 nm transient spectra of the ferric species.

Finally, Fig. 1(d) shows the transient spectrum 70 ps after photoexcitation of $[Fe(CN)_6]^{3-}$ at 266 nm. The transient is reminiscent of Fig. 1(b), but in this case the absorption increase above the edge is more prominent than below it. Indeed, as shown by the black and red dashed traces in Fig. 1(d), neither a red nor a blue shift are able to fully account for the changes around the edge, which would appear to be best described as a broadening of the white line feature (7.132 keV) in the excited state. The differences between the 266 nm and 355 nm excitations for the ferric case (Fig. 2(b)) point to a different photoproduct, which contradicts the conclusions from previous optical studies that the photoproducts of $[Fe(CN)_6]^{3-}$ are wavelength-independent.[13,15] In addition, it is interesting to note that the 266 nm transient of the ferrous species after subtraction of the oxidative contribution (Fig. 2(a)) is, to within the rather large error bars, in agreement to the main features of the 266 nm transient spectrum of the ferric species (Fig. 2(c)). This suggests a common photoproduct to both ferrous and ferric species upon 266 nm excitation.

Obviously, the extracted transient spectra in Fig. 2(a) depend on the precision with which the product $f(t) \cdot \Phi_{po}$ is known. In addition, since an aquated species was predicted[6,7] for 266 nm excitation, and since the transient spectrum in Fig. 2(a) deviates from Fig. 1(a), one may suspect that a poor determination of the $f(t) \cdot \Phi_{po}$ may lead to an incorrect transient spectrum for the second photoproduct. In order to explore this possibility, we have varied the value of $f(t) \cdot \Phi_{po}$ from 2.75% to 4.75% in steps of 0.2% and compared in Figs. S5 and S6,[49] the extracted second product transient spectrum with the aquated product transient from Fig. 1(a). In none of these cases do we see any satisfactory agreement between the two. This, and the fact that the extracted second product transient spectrum agrees with the transient spectrum of the ferric species upon 266 nm excitation convinces us that our fit, based on the minimisation of the sum of square residuals, is indeed consistent.

IV. DISCUSSION

In Section III, we presented the transient spectra of $[Fe(CN)_6]^{4-}$ and $[Fe(CN)_6]^{3-}$ excited at 355 nm and 266 nm. Our results can be summarised as follows: (a) the transient spectra of both species excited at 355 nm exhibit similar features (Figs. 1(a) and 1(b)). (b) The 355 nm transient for $[Fe(CN)_6]^{4-}$ is characterised by three clear spectral changes: (i) a new pre-edge feature at 7.113 keV; (ii) a 1.0 eV red shift of the absorption edge, indicative of a gain in electron density on the iron; and (iii) a negative feature at 7.15 keV in the above ionisation resonance. (c) The 266 nm excitation of the ferrous complex is dominated by the oxidised

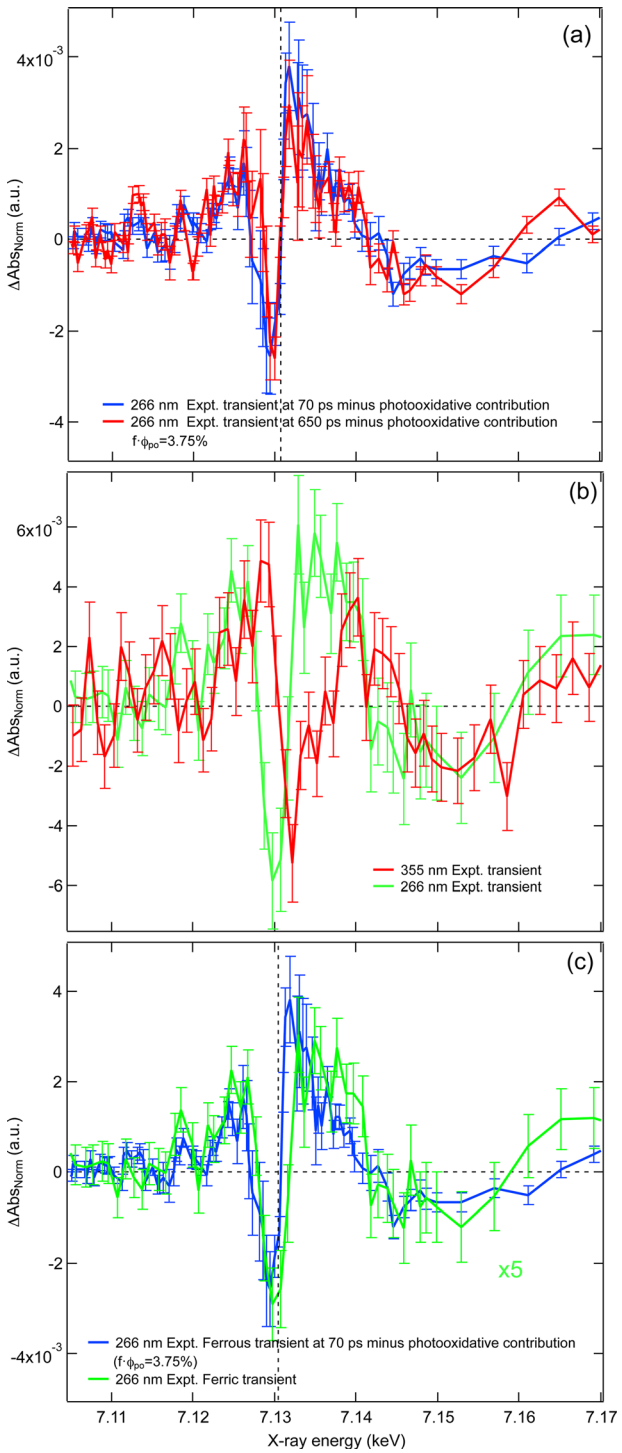

FIG. 2. (a) Comparison of the second photoproduct (once the photo-oxidative component has been removed) transient 70 ps (blue) and 650 ps (red) after 266 nm photoexcitation of $[Fe(CN)_6]^{4-}$. (b) Comparison between the 355 nm and 266 nm transient spectrum of $[Fe(CN)_6]^{3-}$. (c) A comparison between the 266 nm transient spectra of $[Fe(CN)_6]^{4-}$ and $[Fe(CN)_6]^{3-}$.

photoproduct (i.e., formation of the ferric species); (d) after subtracting the latter contribution, a second product appears whose transient is, to within error bars, similar to that of the ferric species observed upon excitation at 266 nm (Fig. 2(c)). This transient is different to that of the aquated species obtained under 355 nm excitation.

In Secs. IV A and IV B, we will discuss these results and analyse them using MS theory and quantum chemistry calculations.

A. 355 nm photoexcitation

In their studies, Shirom and Stein[6,7] concluded that the aquated species $[Fe(CN)_5OH_2]^{3-}$ is characterised by a broad absorption band centred around 450 nm, which appears within 1 ns upon excitation at >310 nm. In a recent ultrafast two-dimensional (2D) UV transient absorption study,[41,43] we found that this band appears within 15 ps with only minor contributions from other photoproducts or $[Fe(CN)_6]^{4-}$ excited states. Given the 70 ps temporal resolution of the present XAS experiments and the previous assignments of the aquated product,[6] we assume that it is the main contributor to the transient spectrum in Fig. 1(a). Here, the increased absorption on the red side of the edge and the drop on its blue side are indicative, as previously mentioned, of an increased electron density at the Fe atom. This is accompanied by the appearance of the pre-edge band at 7.113 keV where a weak band is already present in the ground state spectrum of $[Fe(CN)_6]^{4-}$ and has been assigned to the 1s-3d(e_g) quadrupole transitions. Indeed, in the O_h symmetry of the complex, the d orbitals split into t_{2g} and e_g orbitals, with the t_{2g} orbitals being fully occupied. The enhancement that is observed in the transient can therefore not be due to the creation of a hole in the 3d(e_g) orbitals since they are already empty. Therefore, they can only result from a symmetry breaking that lifts the forbidden character of the quadrupole transitions.

To rationalise these observations, we simulate the difference spectrum that is due to the formation of the aquated species, $[Fe(CN)_5OH_2]^{3-}$ or a pentacyano photoproduct, since both would lead to the loss of octahedral symmetry and an increased electron density at the Fe atom. For the latter, we consider both the C_{4v} and D_{3h} symmetry species, noting that D_{3h} is the minimum energy structure. Fig. 3(a) compares the experimental and simulated transient spectrum for each photoproduct. The agreement for the aquated species is good and captures all of the spectral changes. However, for both pentacyano photoproducts, especially the D_{3h} structure, we observe notable differences with the experimental transient spectrum, in particular, an enhancement of the pre-edge feature and a smaller red shift of the absorption edge. This leads us to rule it out as a significant product on this timescale. An alternative photoproduct which could be considered is the hydroxylated species $[Fe(CN)_5OH]^{4-}$ but under our unbuffered sample conditions we expect the aquated product to be formed. This is consistent with the results of Shirom and Stein who found no dependence on the photoproduct formed over a pH range from 3.8 to 10.5,[6] ruling out a contribution from the hydroxylated species.

The structural properties of the aquated species, identified as the dominant photoproduct, are given in Table I. They show that the water molecule binds to the iron atom at an Fe-O distance of ∼2.2 Å. The bond length of the CN^- *trans* to the water molecule decreases (i.e., forms

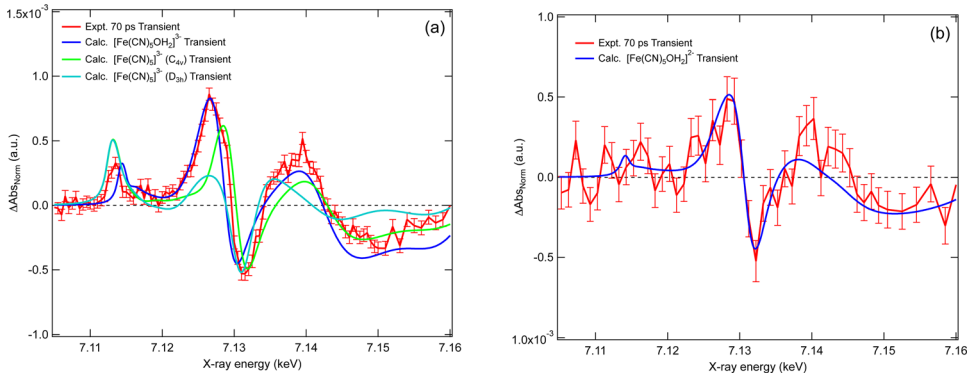

FIG. 3. (a) The experimental (red) 70 ps after 355 nm photoexcitation of $[Fe(CN)_6]^{4-}$ and calculated transient spectra of $[Fe(CN)_5]^{3-}$, C_{4v} (green), $[Fe(CN)_5]^{3-}$, D_{3h} (cyan), and $[Fe(CN)_5OH_2]^{3-}$ (dark blue). (b) The experimental (red) 70 ps after photoexcitation of $[Fe(CN)_6]^{3-}$ at 355 nm and calculated transient spectra of $[Fe(CN)_5OH_2]^{2-}$ (blue).

a stronger bond) by 0.05 Å, while the Fe-C distances for the equatorial CN^- ligands elongate by 0.01 Å. The red shift of the edge, which is quite large, ~1 eV, compared to the 2 eV oxidation state (blue) shift upon oxidation of $[Fe(CN)_6]^{4-}$ is also reproduced. The magnitude of this shift caused by the removal of a CN^- ligand has a strong electron withdrawing effect on the Fe atom through the π-backbonding interaction. Although this is somewhat compensated for by the σ-donation interaction, the strong ligand field effect of the CN^- will result in a significant shift of the spectra as demonstrated by Hocking *et al.*[44] for the $L_{2/3}$-edge of the ferrous and ferric hexacyanides. The H_2O ligand does not have such an effect.

The negative feature in the transient corresponding to the second above ionisation resonance (7.15 keV) in the ground state spectrum is due to the partial loss of the strong focussing contribution of the MS along the linear Fe-CN bond,[36,37,40] which is not compensated for by scattering from the oxygen of the water molecule. Finally, the strong pre-edge feature at 7.113 keV corresponds to transitions into the $d_\sigma(e_g)$ orbitals. As already mentioned, given that the 1s-3d transition is dipole forbidden in the octahedral symmetry of $[Fe(CN)_6]^{4-}$, its intensity increase can only result from a symmetry lowering which is expected upon formation of an aquated species. Indeed, the anticipated C_{4v} symmetry of the latter (neglecting the H atoms of the bound H_2O molecule) favours 3d-4p mixing that introduces a dipole component in the 1s-3d transition. This transition therefore represents a clear signature of the symmetry breaking associated with aquation and is consistent with Westre *et al.*[45] who showed that for a range of iron complexes, the pre-edge intensities for complexes of C_{4v} symmetry, such as $[Fe(CN)_5OH_2]^{3-}$, are ~5–10 times larger than those of octahedral symmetry.

We now turn to the case of the ferric complex. Within the signal-to-noise ratio, the transient spectrum of $[Fe(CN)_6]^{3-}$ excited at 355 nm (Fig. 1(b)) exhibits a similar profile to the $[Fe(CN)_6]^{4-}$ complex (Fig. S3[49]) suggesting the formation of the aquated species, $[Fe(CN)_5OH_2]^{2-}$ as previously proposed.[13] Just as for the ferrous case, the increased absorption on the red side of the edge and the decreased one on the blue side points to a 1.0 eV red shift of the edge (Fig. 1(b), dashed black trace), which reflects an increased electron density on the Fe atom. Fig. 3(b) compares the experimental (red) and calculated (blue) transient spectra, which show good agreement within the signal-to-noise ratio. The red shift of the edge is reproduced as is the negative feature at 7.15 keV. The structural parameters of the ferric aquated species are given in Table I. In this case, we find that the water associates to the iron at an Fe-O distance of ~2.05 Å, significantly shorter than in the ferrous case due to the larger electrostatic attraction between the oxygen and Fe^{3+}. Therefore, although the transient spectra upon 355 nm excitation are similar for the ferrous and ferric complexes, the aquated photoproduct is not the same species. Given the poor signal-to-noise ratio, a pre-edge peak cannot be observed in this case, although it would be expected just on the basis of symmetry breaking arguments. However, there may be additional reasons for it not to be discernible in our transient spectrum. Fig. 4(a) compares the calculated intensity of the $d\sigma$ pre-edge peak in the case of ferrous hexacyanide, its aquated photoproduct, and for two symmetries (C_{4v} and D_{3h}) of the pentacyano complex. In Fig. 4(b), the integrated intensity of the $d\sigma$ pre-edge peak (Fig. 4(a)) for the aquated ferrous complex is plotted as a function of the Fe-O distance. It can be seen that the intensity is strongly sensitive to the latter. This trend is identical for the ferric complex and given that the Fe-O bond distance is 2.05 Å; this is expected to lead to a pre-edge intensity which is approximately half that of the pre-edge peak for the ferrocyanide complex for which the bond distance is 2.2 Å. Together with the poor signal-to-noise ratio, this may be the reason why a pre-edge band does not show up in Fig. 1(b).

Compared to ferrocyanide, the quantum yield for ferricyanide is significantly smaller.[15] The reason for this is likely because 355 nm excitation of $[Fe(CN)_6]^{3-}$ populates a LF ($^2T_{1g}$) and LMCT states, which overlap in the absorption spectrum (Fig. S2(b)[49]). Therefore, although as in the ferrous case, the photoaquation mechanism most probably proceeds via a LF state, which reduces the ligand field stabilisation through the population of the anti-bonding e_g-orbitals, coupling to the LMCT states may provide an additional relaxation channel. In this regards, recent work by Gaffney and co-workers[46] upon 400 nm excitation of the ferric species concluded that this state has a lifetime of 28.1 ps in Dimethyl sulfoxide and 17.5 ps in acetonitrile

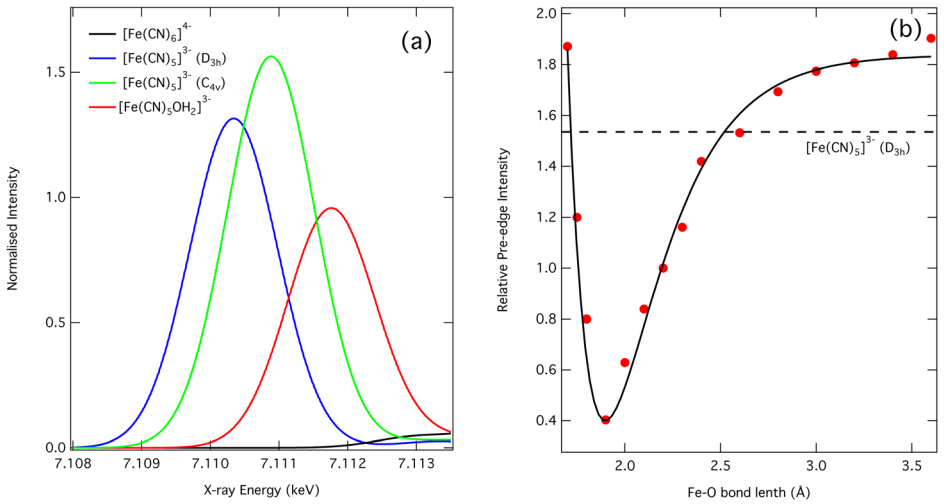

FIG. 4. (a) Intensity of the pre-edge peak of $[Fe(CN)_6]^{4-}$ (black), $[Fe(CN)_5OH_2]^{3-}$ (red), $[Fe(CN)_5]^{3-}$ (blue, D_{3h}), and $[Fe(CN)_5]^{3-}$ (blue, C_{4v}) calculated using time-dependent density functional theory as described in Sec. II C. The intensity has been normalised to the intensity of the $[Fe(CN)_5OH_2]^{3-}$ product. (b) The integrated intensities of the pre-edge feature enhanced by photoaquation, normalised to the calculated intensity of $[Fe(CN)_5OH_2]^{3-}$. This trend is identical for $[Fe(CN)_5OH_2]^{2-}$. The dashed line is the normalised integrated intensities for the D_{3h} $[Fe(CN)_5]^{3-}$ species.

and therefore any population of the LMCT state will return to the ground state within the temporal width of the X-ray pulse and consequently not contribute to our transient spectrum.

B. 266 nm photoexcitation

For the ferrous complex, as expected, the dominant photoproduct is the ferric species (Figs. 1(c) and S4[49]) while an additional photoproduct is present, whose transient was extracted by subtraction of the static ferric-ferrous difference spectrum from the experimental transient (Fig. 2(a)). In their flash photolysis experiments, Shirom and Stein[6,7] found that the yield of photoaquation was lower upon 254 nm excitation (∼0.1) than >313 nm excitation. The 254 nm excitation reaches both the CTTS states and the ligand-field $^1T_{2g}$ state (Fig. S2(a)[49]), which is probably also the case under 266 nm excitation. We would therefore expect an aquated species to arise from the latter. However, as shown in Figs. S5 and S6,[49] even though the extracted spectra (Fig. 2(a)[49]) are somewhat dependent on the photolysis and quantum yields obtained in Fig. 1(c), they remain quite different from those recorded under 355 nm excitation of the ferrous and ferric complexes (Figs. 1(a) and 1(b)). Interestingly, the extracted transients seem closer to the transient spectrum obtained upon 266 nm excitation of the ferric complex (Fig. 2(c)), bearing in mind the large error bars in both transient spectra. This suggests that in addition to photooxidising the ferrous complex, the 266 nm pulse also re-excites the primary ferric photoproduct. This is quite likely under our experimental conditions. Indeed, in order to understand the mechanism of the CTTS mediated electron ejection to the solvent, we carried out a femtosecond fluorescence up-conversion experiment upon 266 nm excitation, similar to a study of the aqueous iodide CTTS states, we recently reported and which yielded a very clear short-lived fluorescence.[47] In the case of $[Fe(CN)_6]^{4-}$, no CTTS fluorescence showed up even though the 266 nm excitation wavelength was more resonant with the CTTS absorption band than in the case of aqueous iodide. Considering that the detection limit in the latter case was ≤60 fs,[47] this implies that the CTTS states of $[Fe(CN)_6]^{4-}$ are quenched by electron ejection on an even shorter time scale. This also agrees with conclusions by Bradforth and co-workers[12] that electron ejection takes place in ≤60 fs. In the present experiment, our pump pulse has a temporal width of ∼10 ps, which means that there is ample time to photooxidise the ferrous complex and re-excite the ferric photoproduct. This scenario is consistent with the spectral evolution for time delays of 70 ps and 650 ps (Fig. 2(a)) because at 70 ps, the spectrum would be expected

to reflect a dominant contribution from the ferric aquated product, formed by re-excitation of the photooxidised product. However, Moggi *et al.*[13] have previously demonstrated that this photoproduct is unstable and, even in the dark, it undergoes reduction to form the ferrous aquated product. In this case, the emergence of the pre-edge at later times (650 ps) would reflect an increased concentration of the reduced ferrous aquated product, which, as previously discussed, has a stronger pre-edge band owing to its Fe-O bond length (Fig. 4(b)). This mechanism would suggest that the 70 ps transient spectrum of the 266 nm excited ferrous complex (after removal of the photo oxidative product) would be in agreement with the 355 nm and 266 nm excitation of the ferric complex, which are not known to lead to photooxidation.[13,15] However, while there are similarities with the 355 nm transient spectrum of the ferric complex, as mentioned both transients excited at 266 nm (Fig. 2(c)) exhibit significant differences in the edge region which do not appear to be consistent with the photoaquated product and appear to contradict previous optical studies that the photoproducts of $[Fe(CN)_6]^{3-}$ are wavelength independent.[13,15] Although 266 nm photoexcitation deposits more energy in the molecule, a direct dissociation of the CN^- ligand to form a pentacyano intermediate is ruled out.

The combination of these two (or more) photoproducts may explain these deviations (Fig. 2(b)). Importantly, the fact that the 266 nm transients of Fig. 2(c) exhibit a pre-edge feature and an enhanced absorption just below the edge points to the formation of a low symmetry product with an increased electron density at the Fe atom, analogous to the 355 nm transients. But this product is clearly not simply the aquated species obtained at 355 nm excitation. This being said, the transients of Figs. 1(b), 1(d), and 2(a) are unfortunately too noisy to conclude what other product or products may be formed under 266 nm excitation. Nevertheless, the mere fact that we obtained different transients under 266 nm and 355 nm excitation of the ferric species points to a reaction channel that involves one of the states lying between 266 and 355 nm or to re-excitation of the primary photoproduct in either case or in both. In the event of a one-photon induced reaction channel, the latter would need to compete with the extremely fast intramolecular electronic relaxation that occurs in such complexes.[48]

V. CONCLUSIONS

We investigated the photoinduced reactions of aqueous ferrous and ferric hexacyanide complexes using picosecond X-ray absorption spectroscopy. From our results, several conclusions have been obtained: (i) following 355 nm excitation of $[Fe(CN)_6]^{4-}$, photoaquation is the principal photo product; (ii) this is also the case in $[Fe(CN)_6]^{3-}$, albeit with a significantly smaller quantum yield, possibly due to the presence of LMCT states; (iii) excitation of $[Fe(CN)_6]^{4-}$ and $[Fe(CN)_6]^{3-}$ at 266 nm excitation yields different transients, demonstrative of different product channels, as expected because the former is dominated by photooxidation, which does not occur in the latter; (iv) extraction of the deviation between the 266 nm transient of $[Fe(CN)_6]^{4-}$ and the *static difference spectrum* yields the transient spectrum of a second product which exhibits changes between 70 and 650 ps. These transients are rather similar to the 266 nm transient spectrum of ferricyanide but differ from the 355 nm excitation of the ferric complex and of the aquated photoproduct following 355 nm excitation of $[Fe(CN)_6]^{4-}$. This suggests that 266 nm excitation of ferrous complexes oxidises the system and re-excites the ferric product. It also point to the formation of more than one photoproduct of which the aquated species may be one of the candidates.

The mechanistic pathways, which lead to the formation of aquated and oxidised species upon excitation of the ferrous complex, have been investigated with femtosecond time resolution using 2D UV spectroscopy and will be reported in a forthcoming publication.[43]

ACKNOWLEDGMENTS

This work was funded by the Swiss NSF through the NCCR MUST 'Molecular ultrafast science and technology' and via Contracts No. 200021_144517, 200020_135502 and 200021_137596. We also thank support from the COST Actions Nos. CM0702, CM1202, and CM1204 via the SBFI Contract Nos. C08.0101 and C13.0062. We are grateful to the staff of the microXAS beamline of the SLS (PSI-Villigen) for their support during the measurements.

[1]E. Amis and J. Hinton, *Solvent Effects on Chemical Phenomena* (Academic Press, New York, 1973).
[2]J. C. Owrutsky, D. Raftery, and R. M. Hochstrasser, Annu. Rev. Phys. Chem. **45**, 519 (1994).
[3]N. Schwentner, C. Bressler, W. Lawrence, J. Xu, and M. Chergui, Chem. Phys. **189**, 205 (1994).
[4]F. Messina *et al.*, Angew. Chem., Int. Ed. **52**, 7043 (2013).
[5]S. J. Greaves *et al.*, Science **331**, 1423 (2011).
[6]M. Shirom and G. Stein, J. Chem. Phys. **55**, 3379 (1971).
[7]M. Shirom and G. Stein, J. Chem. Phys. **55**, 3372 (1971).
[8]P. Rentzepis, R. Jones, and J. Jortner, Chem. Phys. Lett. **15**, 480 (1972).
[9]J.-C. Mialocq, J. Sutton, and P. Goujon, J. Chem. Phys. **72**, 6338 (1980).
[10]S. Pommeret *et al.*, Chem. Phys. Lett. **288**, 833 (1998).
[11]N. A. Anderson, K. Hang, J. B. Asbury, and T. Lian, Chem. Phys. Lett. **329**, 386 (2000).
[12]V. Lenchenkov, J. Kloepfer, V. Vilchiz, and S. E. Bradforth, Chem. Phys. Lett. **342**, 277 (2001).
[13]L. Moggi, F. Bolletta, V. Balzani, and F. Scandola, J. Inorg. Nucl. Chem. **28**, 2589 (1966).
[14]O. Horváth and K. L. Stevenson, *Charge Transfer Photochemistry of Coordination Compounds* (Wiley-VCH, 1993).
[15]M. Fuller, K. Lebrocq, E. Leslie, and I. Wilson, Aust. J. Chem. **39**, 1411 (1986).
[16]K. B. Reddy and R. Van Eldik, Inorg. Chem. **30**, 596 (1991).
[17]Z. Bradić, D. Pavlovic, I. Murati, and S. Asperger, J. Chem. Soc., Dalton Trans. **1974**, 344.
[18]D. A. Estrin *et al.*, Inorg. Chem. **35**, 3897 (1996).
[19]E. F. Aziz, M. H. Rittmann-Frank, K. M. Lange, S. Bonhommeau, and M. Chergui, Nature Chemistry **2**, 853 (2010).
[20]M. I. Finston and H. G. Drickamer, J. Phys. Chem. **85**, 50 (1981).
[21]F. P. Rotzinger, Chem. Rev. **105**, 2003 (2005).
[22]H. Bolvin, J. Phys. Chem. A **102**, 7525 (1998).
[23]M. Chergui, Acta Cryst. **A66**, 229–239 (2010).
[24]T. Penfold, C. Milne, and M. Chergui, Adv. Chem. Phys. **153**, 1 (2013).
[25]F. Lima *et al.*, Rev. Sci. Instrum. **82**, 063111 (2011).
[26]F. Neese *et al.*, *ORCA—An Ab initio, Density Functional and Semiempirical Program Package* (Max Planck Institute for Bioinorganic Chemistry, 2012).
[27]M. Reiher, O. Salomon, and B. A. Hess, Theor. Chem. Acc. **107**, 48 (2001).
[28]S. Sinnecker, A. Rajendran, A. Klamt, M. Diedenhofen, and F. Neese, J. Phys. Chem. A **110**, 2235 (2006).
[29]Y. Joly, Phys. Rev. B **63**, 125120 (2001).
[30]O. Bunău and Y. Joly, J. Phys.: Condens. Matter **21**, 345501 (2009).
[31]S. DeBeer-George, T. Petrenko, and F. Neese, J. Phys. Chem. A **112**, 12936 (2008).
[32]G. Capano *et al.*, Chem. Phys. Lett. **580**, 179 (2013).
[33]F. Lima *et al.*, Phys. Chem. Chem. Phys. **16**, 1617 (2014).
[34]S. Hirata and M. Head-Gordon, Chem. Phys. Lett. **314**, 291 (1999).
[35]S. Debeer-George, T. Petrenko, and F. Neese, Inorg. Chim. Acta **361**, 965 (2008).
[36]A. Bianconi, M. Dell'Ariccia, P. J. Durham, and J. B. Pendry, Phys. Rev. B **26**, 6502 (1982).
[37]M. Obashi, Jpn. J. Appl. Phys., Part 1 **17**, 563 (1978).
[38]K. Hayakawa *et al.*, J. Am. Chem. Soc. **126**, 15618 (2004).
[39]T. Lee, Y. Jiang, C. G. Rose-Petruck, and F. Benesch, J. Chem. Phys. **122**, 084506 (2005).
[40]T. Penfold *et al.*, J. Chem. Phys. **138**, 014104 (2013).
[41]M. Reinhard, "Ultrafast x-ray and 2-dimensional UV spectroscopic Studies of hexacyanoferrate ions in solution," Ph.D. thesis (Ecole Polytechnique Fédérale de Lausanne, Lausanne, 2013).
[42]C. Bressler, R. Abela, and M. Chergui, Z. Kristallogr. **223**, 308 (2008).
[43]M. Reinhard, G. Auböck, and M. Chergui, "Ultrafast 2D UV spectroscopy of photoaquation of aqueous hexacyanoferrate(II) ions," (to be published).
[44]R. Hocking *et al.*, J. Am. Chem. Soc. **128**, 10442 (2006).
[45]T. E. Westre *et al.*, J. Am. Chem. Soc. **119**, 6297 (1997).
[46]W. Zhang, M. Ji, Z. Sun, and K. J. Gaffney, J. Am. Chem. Soc. **134**, 2581 (2012).
[47]F. Messina, O. Braem, A. Cannizzo, and M. Chergui, Nat. Commun. **4**, 2119 (2013).
[48]O. Bräm, F. Messina, A. M. El-Zohry, A. Cannizzo, and M. Chergui, Chem. Phys. **393**, 51 (2012).
[49]See supplementary material at http://dx.doi.org/10.1063/1.4871751 for the ground state iron K-edge and the UV-visible spectra of both complexes, a transient spectrum over an extended energy range of aqueous ferrous cyanide after 266 nm photoexcitation and the effect of the photolysis yield on the transient spectrum presented in Fig. 2a.